Journal of Geochemical Exploration 172 (2017) 109–119

Contents lists available at ScienceDirect

Journal of Geochemical Exploration

journal homepage: www.elsevier.com/locate/gexplo

Fluid geochemical constraints on the heat source and reservoir temperature of the Banglazhang hydrothermal system, Yunnan-Tibet Geothermal Province, China

Qinghai Guo *, Mingliang Liu, Jiexiang Li, Xiaobo Zhang, Wei Guo, Yanxin Wang *

State Key Laboratory of Biogeology and Environmental Geology, Laboratory of Basin Hydrology and Wetland Eco-restoration & School of Environmental Studies, China University of Geosciences, 430074 Wuhan, Hubei, PR China

ARTICLE INFO

Article history:
Received 15 September 2015
Revised 29 April 2016
Accepted 23 October 2016
Available online 24 October 2016

Keywords:
Geothermal water
Geochemistry
Magma chamber
Mixing water
Banglazhang
Yunnan-Tibet Geothermal Province

ABSTRACT

Longling, located in the Yunnan-Tibet Geothermal Province of China, is characterized by the wide distribution of hydrothermal areas, among which the Banglazhang system is the most geothermally active and marked by intensive hydrothermal activities. There is a lack of neutral Cl waters at Banglazhang, and the geothermal waters are mainly Na-HCO_3 type with low but comparable SO_4 and Cl concentrations. The SiO_2 concentrations of the Banglazhang geothermal waters indicate equilibration in a shallow reservoir with a temperature around 150 °C. While dilution by Mg-rich cold groundwaters complicates geothermometry, the Na-K geothermometer suggests that this shallow reservoir is fed by geothermal fluid from a deeper reservoir above 200 °C. The geophysical investigations made in the neighboring regions of Banglazhang indicate that the Banglazhang system is likely to be located above the margin of a comparatively shallow-seated magma chamber. However, the hydrochemical and O, H and S isotopic evidence doesn't imply a mixing of magmatic fluid with Banglazhang geothermal waters. The geochemical scenario below Banglazhang is quite different than some typical magmatic-hydrothermal systems in China (such as Yangbajain and Rehai) where the geochemistry of geothermal waters are strongly affected by the input of magmatic fluid. The efforts made in this study might be suggestive for identifying the geothermal and geochemical origin of a large number of unexplored high-temperature hydrothermal systems in remote Yunnan and Tibet of China whose heat sources and geological conditions are unclear.

1. Introduction

High-temperature hydrothermal systems are widely distributed in western Yunnan Province and Southern Tibet autonomous region of China, also called the Yunnan-Tibet Geothermal Province, which is an important part of the Mediterranean-Himalayas geothermal belt. According to the estimations based upon chemical geothermometers, there are 88 and 129 hydrothermal systems with reservoir temperature higher than 150 °C in Yunnan and Tibet, respectively (Liao and Zhao, 1999). However, the existence of such high-temperature fluids has been evidenced by only two drilling in Yangbajain and Yangyi, where the geothermal fluids are used for electricity generation (Duo, 2003; Guo et al., 2009). It is commonly accepted that, although meteoric water is the major recharge source for all hydrothermal systems in Yunnan and Tibet, the direct magmatic fluid contribution to the geothermal waters is not negligible if we consider three high-temperature systems, i.e. Yangbajain (Tibet), Yangyi (Tibet) and Rehai (Yunnan), where the existence of magma chamber has been confirmed by geophysical and geochemical studies (Bai et al., 1994; Shangguan et al., 2000; Zhao et al., 2002; Guo et al., 2009). Moreover, magmatic heat source also led to the convection of deeply circulating groundwaters, sharply increased their temperatures, and thereby contributed to the formation of these systems.

The Longling County belongs to the Baoshan Prefecture of Yunnan Province and is located very adjacently to Tengchong, the most extensive volcanic geothermal region in China that is composed of 58 hydrothermal areas including Rehai (Tong and Zhang, 1989) (Fig. 1). A great number of hydrothermal areas are distributed in Longling as well, among which Banglazhang, with a total area of around 0.2 km^2, is the largest and most active. The Banglazhang geothermal field is characterized by various hydrothermal manifestations, e.g. hot springs, fumaroles and intensive hydrothermal alteration. In addition, a series of hydrothermal explosions occurred in the northwestern part of the Banglazhang field immediately after the Longling earthquake in 1976,

* Corresponding authors.
E-mail addresses: qhguo2006@gmail.com (Q. Guo), yx.wang1108@gmail.com (Y. Wang).

http://dx.doi.org/10.1016/j.gexplo.2016.10.012
0375-6742/

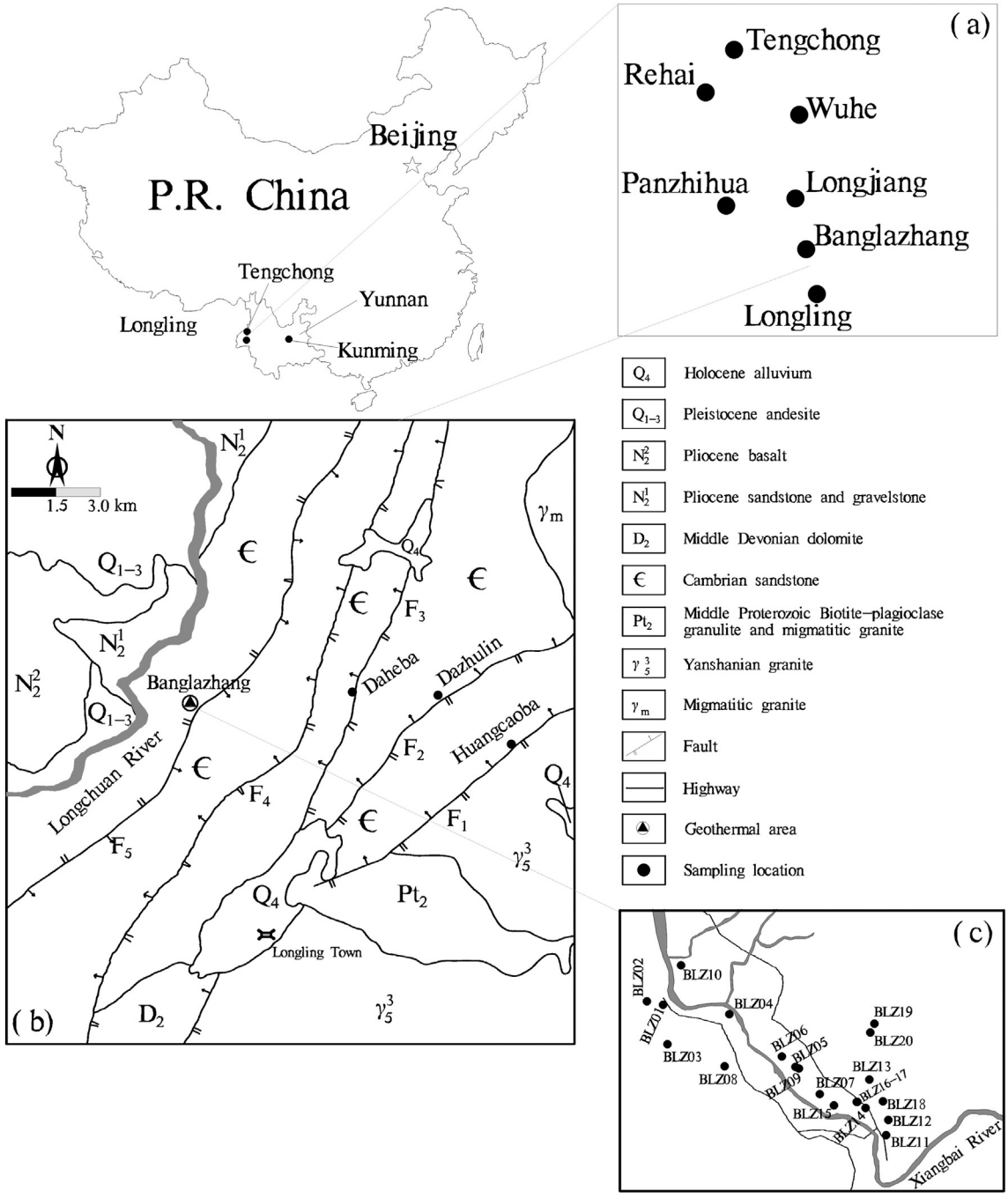

Fig. 1. Simplified geological map of Longling and sampling locations.

which resulted in the formation of a hot spring with the highest outlet temperature (97 °C) among all Banglazhang springs and a small-scale geyser that vanished a few years ago (Liu, 2009).

The subsurface temperatures of Banglazhang calculated by use of common solute geothermometers are generally much higher than those of its neighboring hydrothermal areas (see Section 4.2 for the details). In view of its intense hydrothermal activities and high subsurface temperatures, it was inferred that there might be a magma chamber below Banglazhang (Liu, 2009). However, the Banglazhang geothermal waters are bicarbonate-sodium or bicarbonate-sulfate-sodium types with very low chloride concentrations, distinctively different from those discharged by typical magmatic-hydrothermal systems across the world. The highest $^{3}He/^{4}He$ ratio calculated for Banglazhang gases is 0.96 Ra (where Ra denotes the $^{3}He/^{4}He$ ratio of air: 1.384×10^{-6}), not necessarily indicating a mantle contribution to the Banglazhang system as well (Zhao, 2008). So, is Banglazhang a magmatic-hydrothermal system or just a system discharging geothermal waters with relatively higher temperatures due to their greater circulation depths? Or it is a magma-heated system but the geothermal waters are not affected by magmatic fluid input? To our knowledge, there are only several published Chinese literatures recording the hydrothermal activities at Banglazhang (Zhou et al., 1995; Lin et al., 2006; Zhao, 2008; Liu, 2009). Little is known about the geothermal background of the Banglazhang system; nor is its geological and geochemical origin. Thus, this study aims to clarify the hydrogeological genesis of the Banglazhang geothermal waters and efforts were made to judge if there exists a magma chamber below Banglazhang and if the Banglazhang geothermal waters are affected by the addition of a

hypothetical magmatic fluid. Other objectives include evaluation of the interactions of ascending geothermal waters with local cold groundwaters and identification of the contribution of other secondary reservoir processes to geothermal water chemistry. Though the conclusions drawn in this paper need to be validated by further evidence beyond surface and geochemical investigations, they might still be suggestive for preliminarily identifying the heat sources and geological geneses of the unexplored hydrothermal systems with estimated reservoir temperatures higher than 150 °C in remote Yunnan and Tibet of China, which is vitally important for the efficient management and sustainable exploitation of hydrothermal resources there.

2. Regional setting and geology

The Banglazhang hydrothermal area lies 12 km northwest of Longling town (the seat of the government of Longling County) (Fig. 1), its altitude ranging from 1254 to 1280 m. The Xiangbai River, flowing from east to west through the area and discharging into the Longchuan River, is the major surface water. The climate in the Banglazhang area is subtropical monsoon type, with a mean annual air temperature of 16.9 °C. In this study, Banglazhang is the main area for geothermal water sampling. In addition, three hydrothermal areas (Daheba, Dazhulin and Huangcaoba) quite near to Banglazhang with much smaller total areas and lower water temperatures were also investigated. Only several low- to middle-temperature hot springs were found in these areas (sampling temperatures are lower than 65 °C) during our field investigation. Detailed geological maps for these areas are not available. The hot springs discharged from Daheba, Dazhulin and Huangcaoba were sampled for comparison with those from Banglazhang.

There are more than 600 hot springs with temperatures over a range of 32 to 97 °C at Banglazhang, and the total discharge of these springs is up to 15 L/s. However, most hot springs have discharge rates much lower than 0.1 L/s, which have been collected by a local piping system for bathing and therefore were impossible to be sampled during the field work of this study. Nevertheless, the hot springs with relatively large discharge rates were still available for sampling and have been collected for chemical and isotopic analyses.

The bedrocks outcropping in the study area comprise Holocene alluvium, Pliocene sandstone and gravelstone, Middle Devonian dolomite, Cambrian quartz sandstone and feldspar sandstone, and Middle Proterozoic Biotite-plagioclase granulite and migmatitic granite. Magmatic rocks including Himalayan andesite and basalt and Yanshanian granite were also distributed (Fig. 1). There are so far no boreholes drilled in Banglazhang, but the host rocks of the Banglazhang system are very likely to be Proterozoic metamorphic rocks according to the surface geology shown in Fig. 1. It is worth noting that the surface hydrothermal manifestations in both Banglazhang and other hydrothermal areas (Daheba, Dazhulin or Huangcaoba) are located at the conjunctions between the Xiangbai River valley in nearly east-west direction and a group of northeast-southwest trending faults (Fig. 1), suggesting that all these hydrothermal systems are fault-controlled. To better understand the geological and hydrogeochemical characteristics of the Banglazhang hydrothermal system, its reservoir lithology, highest subsurface temperature, hydrochemical type and major discharge path were compared with those of Yangbajain and Rehai (Guo et al., 2007; Guo and Wang, 2012), two representative high-temperature, magmatic-hydrothermal systems in southern Tibet and western Yunnan, respectively. The summary of these geochemical and geological data is reported in Table 1.

3. Materials and methods

3.1. Field sampling and measurements

Water samples from 27 sites were collected in June 2013, among which 18 hot spring samples were collected from the Banglazhang hydrothermal area and 6 from its neighboring hydrothermal areas: Daheba, Dazhulin and Huangcaoba. In addition, 2 and 1 cold springs were also sampled at Banglazhang and Dazhulin, respectively. The sampling sites of all water samples are presented in Fig. 1 while their sampling information, in-situ parameters and hydrochemical types are reported in Table 2.

All water samples were filtered through 0.45 μm membrane on site. Samples were stored in 300 mL polyethylene bottles which had been soaked in high-purity trace metal-free 5% HCl and rinsed three times with distilled water before sampling. For cation analysis, reagent-grade HNO_3 with molar concentration up to 14 M was added to one sample collected at each site to bring pH below 1. For SiO_2 analysis, the samples were diluted ten-fold using deionized water to prevent SiO_2 precipitation. For Al analysis samples ultrafiltration was obtained by a 0.2 μm membrane. Samples splits for analyses of anions and stable water isotopes (δD and $\delta^{18}O$) were stored without any addition of chemical agents. For sulfur isotope analysis the sulfate and sulfide in water samples were precipitated as $BaSO_4$ and CdS on site by use of $BaCl_2$ and $Cd(CH_3COO)_2$, respectively. Water temperature and pH, as unstable parameters, were measured with hand-held meters that were calibrated prior to sampling. H_2S was determined in situ using an HACH colorimeter. Total alkalinity was measured using the Gran titration method on the sampling day, based on which the concentrations of HCO_3^-, CO_3^{2-} and CO_2 in all samples were calculated using PHREEQC code incorporating WATEQ4F database (Parkhurst and Appelo, 1999).

3.2. Lab analysis and data processing

3.2.1. Measurements of anions and cations as well as oxygen, hydrogen and sulfur isotopes

The SO_4^{2-}, Cl^-, F^- and Br^- concentrations were determined on an unacidified sample by ion chromatography. Bromide is below the detection limit of 0.03 mg/L in all samples and, for this reason, is not reported. The concentrations of Na, K, Ca, Mg, Li, Sr, Ba, Al, Fe, Si, B, As and Se were analyzed by ICP-OES, and those of Rb, Cs and Sb by ICP-MS within 2 weeks after sampling.

The CO_2 equilibration method was used for the measurement of $^{18}O/^{16}O$ ratio of water samples, while for D/H ratio, the H_2 was generated by the Zn-reduction method (Coleman et al., 1982). Isotope ratios of CO_2 and H_2 were measured on a Finnigan MAT-251 mass spectrometer, and the fractionation factor between CO_2 and water at 25 °C was

Table 1
Comparison of geological and geochemical characteristics among the Banglazhang (this study), Yangbajing (Guo et al., 2007) and Rehai (Guo and Wang, 2012) hydrothermal systems. Note that the highest subsurface temperature is estimated by use of K-Mg geothermometer, and the number in the parenthesis for the Yangbajing hydrothermal system is the measured temperature of geothermal well ZK4001 at depth of 1125 m (Duo, 2003).

Hydrothermal system	Reservoir lithology	Highest subsurface temperature (°C)	Hydrochemical type of geothermal water	Major discharge path	Deep reservoir
Banglazhang	Proterozoic metamorphic rocks	160	$Na\text{-}HCO_3$	Geothermal springs	unproven
Yangbajing	Himalayan granite	225 (255)	Na-Cl	Geothermal production wells	proven
Rehai	Yanshanian granite and Proterozoic metamorphic rocks	269	$Na\text{-}HCO_3\text{-}Cl$	Geothermal springs	proven

Table 2
Characteristics of water samples (Sampling temperature in °C and TDS in mg/L).

No.	Sample type	Sampling location	Sampling T	pH	TDS	Hydrochemical type
BLZ01	Hot spring	Banglazhang	97.0	8.54	684	Na-HCO3
BLZ02	Hot spring	Banglazhang	72.6	8.15	665	Na-HCO3-SO4
BLZ03	Hot spring	Banglazhang	62.9	7.29	731	Na-HCO3-SO4
BLZ04	Hot spring	Banglazhang	66.5	8.10	503	Na-HCO3
BLZ05	Hot spring	Banglazhang	52.0	8.67	736	Na-HCO3
BLZ06	Hot spring	Banglazhang	94.4	8.48	743	Na-HCO3
BLZ07	Hot spring	Banglazhang	77.1	7.62	710	Na-HCO3
BLZ08	Hot spring	Banglazhang	60.5	6.55	267	Na-HCO3
BLZ09	Hot spring	Banglazhang	85.8	7.61	758	Na-HCO3-SO4
BLZ10c	Cold spring	Banglazhang	23.9	8.37	130	Ca-Na-HCO3
BLZ11	Hot spring	Banglazhang	82.4	7.97	687	Na-HCO3
BLZ12	Hot spring	Banglazhang	58.9	7.91	697	Na-HCO3
BLZ13	Hot spring	Banglazhang	46.6	6.80	265	Na-HCO3
BLZ14	Hot spring	Banglazhang	87.4	8.59	733	Na-HCO3
BLZ15	Hot spring	Banglazhang	76.5	7.27	749	Na-HCO3
BLZ16	Hot spring	Banglazhang	70.7	7.74	705	Na-HCO3
BLZ17	Hot spring	Banglazhang	93.3	8.09	588	Na-HCO3
BLZ18	Hot spring	Banglazhang	73.3	7.00	625	Na-HCO3
BLZ19c	Cold spring	Banglazhang	21.1	8.71	106	Ca-Mg-HCO3
BLZ20	Hot spring	Banglazhang	32.8	8.70	337	Na-HCO3
DHB01	Hot spring	Daheba	55.2	6.95	430	Na-Ca-HCO3
DHB02	Hot spring	Daheba	56.9	6.87	443	Na-Ca-HCO3
DZL01	Hot spring	Dazhulin	55.6	7.75	242	Na-HCO3
DZL02c	Cold spring	Dazhulin	20.3	7.62	66	Ca-Na-HCO3
HCB01	Hot spring	Huangcaoba	50.4	8.33	183	Na-HCO3
HCB02	Hot spring	Huangcaoba	53.0	8.39	191	Na-HCO3
HCB03	Hot spring	Huangcaoba	61.0	8.23	199	Na-HCO3

assumed to be 1.0412 (Coplen, 1993). The reproducibility of water isotope measurements is ±0.1‰ for $\delta^{18}O$ and ±0.5‰ for δD. The oxygen-18 and deuterium values were expressed in usual notation of δ ‰ vs. V-SMOW (Vienna-Standard Mean Ocean Water) where $\delta = 1000\,(R_{sample}/R_{SMOW} - 1)$ and $R = {}^{18}O/{}^{16}O$ or D/H.

For sulfur isotopic analysis the precipitates obtained in the field were recovered by centrifugation, then were washed and dried beforehand. Prior to further treatment, CdS was converted to $BaSO_4$ by the semi-melting method with Na_2CO_3-ZnO at 850 °C. The conversion of $BaSO_4$ to SO_2 was completed via high-temperature combustion along with SiO_2 and V_2O_5 at 980 °C. Sulfur isotope ratios were determined by use of Finnigan MAT-251 mass spectrometer and expressed in per mil (‰) with conventional delta-notation (δ) as well. The $\delta^{34}S$ values of sulfate or sulfide in water samples are reported relative to the Canyon Diablo Troilite standard ($\delta^{34}S$-CDT = 0‰). Quality control on sulfur isotope measurements was carried out based on international standard NBS 127 and lab standard LTB-2 whose measured $\delta^{34}S$ values in this study were 20.22‰ and 1.84‰ respectively. Duplicate preparations and analyses of $\delta^{34}S$ agreed within ±0.2‰.

The concentrations of measured chemical constituents and their standard deviations are summarized in Table 3 and Table 4, respectively. The isotopic data are presented in Table 5. The charge imbalances of all water samples were calculated and listed in Table 3 as well. The geothermal water samples collected in this study, especially those from Banglazhang, are generally of high analytical accuracy, and the charge imbalances of most samples are less than or around 10%.

3.2.2. Calculation of O- and H-isotopic fractionation as a result of near-surface boiling

Hot springs with sampling temperatures very close to local boiling point are usually the evidence of geothermal fluid's adiabatic cooling at near-surface. In this case the oxygen-18 and deuterium compositions of subsurface fluids need to be estimated from those measured for the corresponding surface springs. Taking into account that the isotopic equilibrium between liquid and vapor phases can generally occur when geothermal fluid boils at the subsurface, we assume that the distribution of oxygen-18 and deuterium between geothermal water and separated vapor within the Banglazhang system is very close to equilibrium. Moreover, although vapor separation may theoretically occur as single step or a continuous boiling process, actual boiling in the subsurface is often at an intermediate phase between two extremes, where the former is the predominant. Hence, the following equation given by Truesdell et al. (1977) was used for water isotopic fractionation

Table 3
Concentrations of chemical constituents in water samples (in mg/L). n.a.: not analyzed; n.d.: not detected.

No.	Alkalinity	SO_4^{2-}	Cl^-	F^-	Na	K	Ca	Mg	SiO_2	Li	Rb	Cs	Sr	Ba	Al	Fe	B	As	Sb	Se	H_2S	Charge imbalance
BLZ01	360	63.3	34.7	24.3	205	15.9	2.68	0.07	124	2.51	0.32	0.64	0.062	0.014	0.25	0.062	3.56	0.141	0.022	0.008	3.50	−4.6%
BLZ02	315	92.8	33.0	27.0	182	14.0	4.27	0.38	117	2.34	0.30	0.63	0.044	0.011	0.17	0.019	3.51	0.160	0.024	0.018	1.50	−8.9%
BLZ03	350	142	28.8	18.6	173	16.7	23.5	2.50	106	2.47	0.33	0.61	0.466	0.020	0.24	0.101	2.52	0.068	0.020	n.d.	n.d.	−9.6%
BLZ04	270	59.4	28.3	16.0	136	10.5	2.00	0.09	85.0	1.56	0.22	0.43	0.018	0.020	0.12	0.014	2.31	0.071	0.032	0.018	2.75	−12.0%
BLZ05	425	72.3	32.9	24.9	214	14.2	1.23	0.05	120	2.98	0.29	0.58	0.004	0.012	0.13	0.013	3.60	0.122	0.032	0.013	4.80	−9.4%
BLZ06	435	72.0	33.2	25.4	213	16.3	1.37	0.09	125	2.80	0.33	0.64	0.008	n.d.	0.42	0.122	3.58	0.094	0.020	0.023	8.75	−10.4%
BLZ07	400	66.8	32.4	24.7	192	17.5	2.90	0.12	126	2.65	0.37	0.76	0.018	n.d.	0.67	0.156	3.50	0.092	0.023	0.013	5.00	−10.5%
BLZ08	160	21.6	7.09	6.13	59.8	6.11	9.01	1.18	56.4	0.66	0.11	0.21	0.076	n.d.	n.d.	0.180	0.86	0.023	0.028	0.009	n.d.	−10.2%
BLZ09	390	115	33.1	24.5	209	16.1	7.22	0.41	117	2.93	0.35	0.71	0.025	0.005	2.42	0.953	3.55	0.107	0.021	n.d.	5.25	−8.1%
BLZ10c	102.5	7.74	5.17	0.56	13.1	2.29	22.2	2.81	15.0	0.04	0.01	0.015	0.089	0.012	0.36	0.210	0.10	0.001	0.024	0.014	n.d.	−8.7%
BLZ11	392.5	61.2	32.7	23.6	187	17.2	2.50	0.15	121	2.58	0.37	0.73	0.022	0.008	0.12	0.088	3.31	0.145	0.033	0.019	3.50	−10.9%
BLZ12	412.5	51.8	32.2	24.6	190	17.2	0.93	0.05	124	2.64	0.36	0.72	0.017	n.d.	0.14	0.006	3.38	0.073	0.022	0.011	4.25	−11.5%
BLZ13	172.5	12.9	8.01	6.21	64.4	5.39	7.37	0.56	52.7	0.72	0.08	0.12	0.046	0.029	0.014	0.009	0.99	0.023	0.027	0.016	n.d.	−10.5%
BLZ14	435	62.3	33.3	25.9	208	19.2	1.44	0.17	128	2.85	0.40	0.77	0.026	0.007	0.70	0.065	3.70	0.087	0.016	0.022	8.50	−10.3%
BLZ15	410	80.6	33.8	26.3	201	18.8	1.69	0.14	131	2.72	0.40	0.76	0.023	0.008	0.32	0.035	3.64	0.168	0.025	0.005	3.50	−11.3%
BLZ16	407.5	53.5	32.5	25.3	192	17.9	1.45	0.05	129	2.62	0.38	0.73	0.014	0.006	0.20	0.011	3.50	0.137	0.022	0.021	3.25	−10.7%
BLZ17	325	45.0	34.6	20.5	156	22.8	1.93	0.20	109	2.11	0.35	0.64	0.016	0.018	0.25	0.071	2.90	0.104	0.020	0.008	5.25	−9.8%
BLZ18	385	28.6	25.0	8.28	183	17.5	6.16	1.83	114	2.59	0.37	0.71	0.054	0.010	0.19	0.028	3.32	0.082	0.023	0.016	n.a.	−1.0%
BLZ19c	92.5	5.48	4.28	0.14	3.2	1.11	21.8	6.08	8.7	0.003	0.01	0.007	0.058	0.029	0.39	0.351	0.03	0.017	0.026	0.014	n.a.	−7.8%
BLZ20	212.5	36.3	9.26	8.12	80.6	30.6	7.42	1.53	34.9	0.61	0.56	0.55	0.080	0.026	0.54	0.163	1.42	0.023	0.003	0.012	n.a.	−7.2%
DHB01	307.5	44.9	23.3	5.76	83.5	9.09	39.3	8.22	25.8	0.68	0.11	0.22	0.337	0.142	0.026	0.126	1.62	0.038	0.025	0.034	0.30	−10.1%
DHB02	315	49.9	24.2	6.01	85.4	9.26	38.0	8.03	26.7	0.69	0.12	0.23	0.343	0.134	n.d.	0.005	1.68	0.031	0.025	0.007	n.a.	−11.8%
DZL01	137.5	33.0	8.53	7.39	66.5	2.35	4.04	0.07	35.5	0.30	0.04	0.07	0.033	0.009	0.037	0.008	0.90	0.025	0.030	0.038	n.d.	−11.9%
DZL02c	37.5	5.55	4.31	0.32	7.3	1.51	7.79	0.50	16.2	0.01	0.003	0.001	0.036	0.012	0.037	0.052	0.003	0.017	0.023	0.017	n.d.	−11.9%
HCB01	112.5	16.1	5.41	8.09	52.4	0.96	2.88	0.04	29.9	0.15	0.02	0.027	0.023	0.016	0.140	0.039	0.21	0.023	0.029	0.015	1.30	−12.0%
HCB02	120	16.3	5.40	8.73	56.3	0.92	2.31	0.01	29.2	0.16	0.02	0.024	0.021	0.008	0.044	0.006	0.23	0.011	0.027	0.006	n.a.	−12.4%
HCB03	125	17.7	5.68	9.05	56.7	1.09	2.21	0.03	30.9	0.17	0.02	0.026	0.021	0.005	0.020	0.003	0.23	0.014	0.028	0.010	1.20	−14.3%

Table 4
Standard deviations of the analytical results of chemical constituents in water samples. N/A: not applicable.

No.	Alkalinity	SO_4^{2-}	Cl^-	F^-	Na	K	Ca	Mg	SiO_2	Li	Rb	Cs	Sr	Ba	Al	Fe	B	As	Sb	Se	H_2S
BLZ01	1.4	2.3	1.1	0.3	3.1	1.1	0.1	0.01	3.7	0.40	0.02	0.02	0.020	0.001	0.03	0.005	0.12	0.008	0.002	0.002	0.21
BLZ02	2.8	2.1	0.3	2.0	9.3	0.4	0.0	0.03	5.4	0.22	0.04	0.03	0.007	0.001	0.01	0.002	0.16	0.011	0.001	0.002	0.07
BLZ03	2.8	0.8	0.1	0.7	3.4	0.6	0.6	0.04	6.8	0.18	0.02	0.09	0.017	0.003	0.01	0.008	0.16	0.008	0.003	N/A	N/A
BLZ04	4.2	1.1	0.7	0.7	0.9	0.6	0.2	0.01	3.0	0.03	0.04	0.02	0.005	0.003	0.01	0.002	0.10	0.002	0.006	0.003	0.07
BLZ05	2.8	1.7	1.4	0.8	1.7	0.1	0.1	0.01	5.6	0.37	0.02	0.04	0.001	0.004	0.02	0.002	0.16	0.010	0.003	0.002	0.14
BLZ06	4.2	1.0	1.0	1.1	9.7	0.3	0.1	0.01	5.3	0.07	0.01	0.01	0.006	N/A	0.06	0.015	0.14	0.006	0.004	0.003	0.21
BLZ07	2.8	1.8	0.8	0.8	6.0	0.3	0.3	0.02	3.6	0.08	0.04	0.10	0.007	N/A	0.08	0.005	0.13	0.004	0.003	0.002	0.14
BLZ08	1.4	1.0	0.1	0.0	2.4	0.2	0.3	0.08	1.7	0.06	0.02	0.02	0.012	N/A	N/A	0.004	0.06	0.001	0.004	0.000	N/A
BLZ09	2.8	6.2	1.2	0.4	4.7	1.0	0.2	0.02	5.2	0.41	0.04	0.07	0.006	0.000	0.11	0.054	0.12	0.008	0.002	N/A	0.00
BLZ10c	2.1	0.1	0.2	0.0	1.6	0.1	1.1	0.08	1.0	0.02	0.00	0.001	0.012	0.000	0.04	0.008	0.02	0.000	0.006	0.004	N/A
BLZ11	3.5	0.3	1.6	0.6	5.9	0.3	0.1	0.02	1.0	0.27	0.02	0.09	0.003	0.001	0.02	0.006	0.07	0.007	0.004	0.003	0.35
BLZ12	0.7	2.5	0.5	0.7	4.3	0.6	0.1	0.02	5.3	0.05	0.09	0.11	0.003	N/A	0.02	0.002	0.06	0.006	0.004	0.003	0.07
BLZ13	2.1	0.6	0.1	0.2	3.4	0.1	0.4	0.04	2.8	0.09	0.02	0.02	0.006	0.006	0.003	0.001	0.08	0.005	0.003	0.002	N/A
BLZ14	2.8	3.0	1.4	0.7	6.2	1.1	0.1	0.02	3.6	0.05	0.02	0.03	0.008	0.001	0.07	0.004	0.21	0.009	0.002	0.003	0.07
BLZ15	2.8	4.5	1.3	0.9	7.8	0.3	0.1	0.01	2.0	0.03	0.03	0.01	0.006	0.004	0.06	0.003	0.03	0.013	0.009	0.002	0.14
BLZ16	3.5	2.2	0.8	0.6	4.3	1.0	0.1	0.01	3.6	0.06	0.02	0.00	0.004	0.000	0.03	0.002	0.16	0.002	0.002	0.003	0.21
BLZ17	1.4	1.2	0.3	0.4	3.8	0.8	0.1	0.02	8.9	0.01	0.05	0.04	0.005	0.001	0.02	0.006	0.10	0.008	0.005	0.002	0.35
BLZ18	1.4	1.6	0.2	0.2	1.8	0.3	0.6	0.03	3.8	0.33	0.03	0.03	0.002	0.003	0.03	0.002	0.07	0.002	0.001	0.002	N/A
BLZ19c	0.7	0.2	0.1	0.0	0.1	0.1	0.6	0.05	0.6	0.002	0.00	0.002	0.011	0.002	0.06	0.015	0.00	0.002	0.001	0.003	N/A
BLZ20	2.1	2.0	0.4	0.2	4.5	0.7	0.4	0.03	1.3	0.08	0.05	0.05	0.010	0.003	0.03	0.004	0.11	0.002	0.000	0.001	N/A
DHB01	2.1	1.6	0.5	0.3	0.9	0.4	3.0	0.01	0.7	0.10	0.02	0.03	0.050	0.006	0.003	0.009	0.02	0.004	0.006	0.006	0.07
DHB02	1.4	1.8	0.5	0.2	2.0	0.0	2.7	0.02	1.8	0.15	0.04	0.03	0.037	0.015	N/A	0.001	0.08	0.004	0.004	0.001	N/A
DZL01	0.7	1.1	0.5	0.3	0.5	0.1	0.1	0.01	2.3	0.03	0.01	0.02	0.007	0.002	0.004	0.001	0.12	0.002	0.004	0.004	N/A
DZL02c	0.7	0.1	0.2	0.0	0.3	0.1	0.5	0.05	1.1	0.00	0.00	0.000	0.008	0.003	0.001	0.005	0.001	0.001	0.004	0.002	N/A
HCB01	0.7	0.9	0.1	0.4	0.4	0.0	0.2	0.01	0.7	0.04	0.01	0.005	0.005	0.002	0.016	0.004	0.02	0.004	0.003	0.003	0.28
HCB02	2.8	0.3	0.3	0.2	2.5	0.0	0.1	0.00	2.2	0.04	0.00	0.008	0.004	0.001	0.008	0.002	0.02	0.001	0.006	0.000	N/A
HCB03	1.4	1.0	0.2	0.3	0.4	0.1	0.2	0.01	2.9	0.02	0.02	0.003	0.001	0.002	0.004	0.001	0.03	0.002	0.003	0.003	0.14

calculation resulting from a boiling process:

$$\delta_{GF} = \delta_{WS} - (1000 + \delta_{WS})(1-\theta) \quad (1)$$

where δ_{GF} and δ_{WS} are the isotopic compositions of geothermal water before and after boiling respectively. θ is a parameter that can be calculated by use of the formula as below:

$$\theta = 1 - \beta + \beta/\alpha \quad (2)$$

α is the fractionation coefficient of oxygen-18 or deuterium between liquid and vapor phases at separation pressure (or temperature), and β is the ratio of vapor in flashing geothermal water expressed as follows:

$$\beta = \frac{H_f - H_w}{H_g - H_w} \quad (3)$$

H_f, H_w and H_g are the enthalpy values of geothermal water before and after vapor separation as well as geothermal vapor, respectively.

In this study, the δD and $\delta^{18}O$ values of samples BLZ01 and BLZ06 with sampling temperatures of 97.0 and 94.4 °C are corrected with the above procedures. The results are presented in Table 5 as well.

3.3. Estimation of reservoir temperatures using SolGeo

A computer program Solute Geothermometers (SolGeo) developed by Verma et al. (2008) was used for estimating the reservoir temperatures in this study. There are a bunch of advantages of SolGeo with respect to reservoir or fluid temperature calculation. It is able to check the validity of the data in its input file and to avoid possible input errors. SolGeo is also capable of converting the concentrations of the chemical variables to the units suitable for the included geothermometers by use of updated, more accurate atomic weights and geothermal water

Table 5
Isotopic composition of hydrogen, oxygen, and dissolved sulfate and sulfide in water samples (in ‰). Stable oxygen and hydrogen isotopic ratios are expressed in δ‰ versus Vienna-standard Mean Ocean Water (V-SMOW). The $\delta^{18}O$ and δD values of samples BLZ01 and BLZ06 were also corrected to those before their near-surface boiling and presented in the parentheses. The $\delta^{34}S$ values of sulfate or sulfide are reported relative to the Canyon Diablo Troilite standard ($\delta^{34}S$-CDT = 0‰). n.a.: not analyzed.

No.	δD	$\delta^{18}O$	$\delta^{34}S$-sulfate	$\delta^{34}S$-sulfide
BLZ01	−77 (−79)	−10.6 (−11.1)	8.5	3.1
BLZ02	−76	−10.7	8.3	6.2
BLZ03	−77	−11.4	n.a.	n.a.
BLZ05	n.a.	n.a.	16.0	1.5
BLZ06	−78 (−80)	−11.5 (−12.0)	14.0	2.7
BLZ07	−78	−11.4	11.1	4.6
BLZ08	−73	−11.1	n.a.	n.a.
BLZ10c	−67	−10.6	13.6	n.a.
BLZ12	−80	−11.8	n.a.	n.a.
BLZ14	−78	−11.4	15.5	3.5
BLZ15	−75	−10.4	10.8	n.a.
BLZ19c	−66	−10.9	n.a.	n.a.
BLZ20	−77	−11.8	n.a.	n.a.
DHB02	−78	−11.9	14.9	n.a.
DZL01	−78	−11.9	11.5	n.a.
DZL02c	−69	−11.1	13.3	n.a.
HCB03	−80	−13.4	12.4	n.a.

Table 6
Reservoir temperatures (in °C) estimated by use of Na/K, K/Mg and quartz geothermometers. [a]: Error indicates an estimation of total propagated errors for the quartz temperatures.

No.	Na/K	K/Mg	Quartz	Error [a]	No.	Na/K	K/Mg	Quartz	Error [a]
BLZ01	212.6	148.7	149.7	1.3	BLZ14	226.1	140.0	151.7	1.3
BLZ02	212.4	117.7	146.4	1.2	BLZ15	226.9	142.9	152.9	1.3
BLZ03	229.2	95.8	140.7	1.2	BLZ16	226.5	159.8	152.0	1.3
BLZ04	212.5	131.3	128.5	1.1	BLZ17	264.5	143.9	141.9	1.2
BLZ05	201.5	151.9	147.5	1.2	BLZ18	228.8	101.3	144.9	1.2
BLZ06	211.6	146.3	150.1	1.3	BLZ20	367.4	120.1	86.6	0.9
BLZ07	224.8	143.1	150.6	1.3	DHB01	239.2	66.2	74.1	0.8
BLZ08	234.0	79.7	108.1	1.0	DHB02	238.8	66.8	75.4	0.8
BLZ09	212.2	120.7	146.1	1.2	DZL01	160.9	91.0	87.3	0.9
BLZ11	225.8	138.6	148.0	1.2	HCB01	125.3	74.9	80.2	0.8
BLZ12	224.1	159.1	149.4	1.3	HCB02	120.1	87.2	79.1	0.8
BLZ13	218.5	85.9	104.9	0.9	HCB03	127.6	83.5	81.5	0.8

density (Verma et al., 2008). Thus the application of SolGeo is helpful for minimizing the errors that occur when the corresponding geothermometric equations are directly employed.

The subsurface temperatures of the study areas calculated using SolGeo are listed in Table 6. The total propagated errors for the obtained Quartz temperatures are also presented in Table 6, which were estimated based on the relative standard deviations for the SiO_2 concentrations of the geothermal water samples.

3.4. Regression analysis

Weighted least-squares regression model was used to explore the relations between the constituents in the water samples. As suggested by Verma (2012), it is not suitable to interpret geochemical data by use of conventional OLS linear regression model, although its correlation coefficient is useful for non-compositional data. Therefore, the hydrogeochemical compositions of water samples as well as their ratios obtained in this study, as typical compositional data, were analyzed using weighted least-squares regression model.

4. Results and discussion

4.1. Hydrochemical and isotopic characteristics

In the Banglazhang hydrothermal area, the hydrochemical types of geothermal waters are basically Na-HCO_3 except for three samples being Na-HCO_3-SO_4 (Table 2). They are characterized with moderate to high spring vent temperatures (46.6–97.0 °C except for a 32.8 °C spring) and neutral to slightly alkaline pH values (6.55–8.70). All geothermal water samples contain HCO_3^- and Na^+ as predominant anion and cation, respectively, whereas their Cl, Ca and Mg concentrations are low with averages values of 28.0, 4.73 and 0.53 mg/L, respectively. The concentrations of F in the Banglazhang geothermal waters are remarkably high (6.1–27.0 mg/L with an average value of 20.0 mg/L). Boron, Li, Rb and Cs concentration ranges (0.86–3.70 mg/L, 0.61–2.98 mg/L, 0.08–0.56 mg/L and 0.12–0.77 mg/L, respectively) are also much higher than those of the local cold groundwaters. Another significant geochemical feature of the Banglazhang samples is their much higher SO_4-Cl molar ratios as compared to those from several representative high-temperature geothermal fields in China, such as Yangbajain and Rehai (Guo et al., 2007; Guo and Wang, 2012) (see Fig. 2). In contrast to the geothermal waters sampled at Banglazhang sites, those collected from Daheba, Dazhulin and Huangcaoba have lower TDS values. Moreover, the Cl-B and Cl-F ratios of the Banglazhang geothermal samples (except for BLZ18) are quite close, whereas those of other geothermal water samples and cold groundwater samples show a wide range of variability.

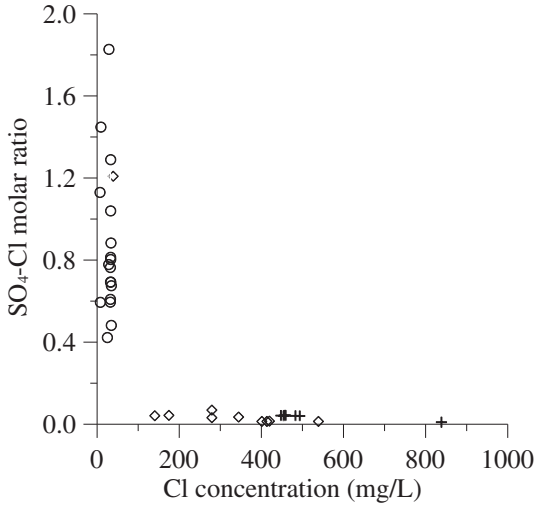

Fig. 2. Plot of SO_4-Cl molar ratio vs. Cl concentration of the geothermal waters from Banglazhang (this study), Yangbajing (Guo et al., 2007) and Rehai (Kharaka and Mariner, 1989). Legend of sample symbols: ○ Banglazhang samples; + Yangbajing samples; ◇ Rehai samples.

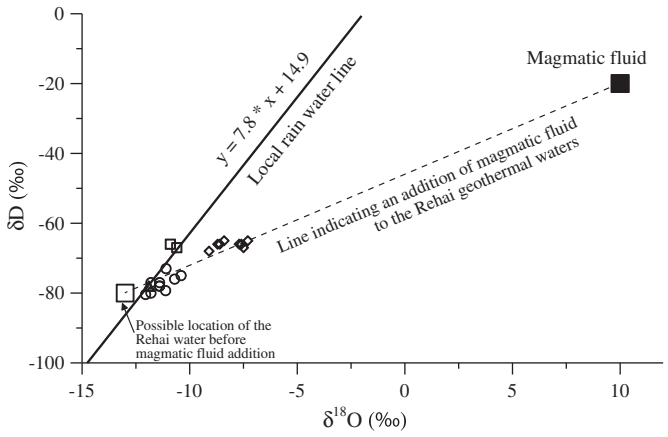

Fig. 3. Plot of δD vs. $\delta^{18}O$ of the Banglazhang water samples. The Rehai geothermal water samples were also plotted for comparison. Legend of sample symbols: ○ geothermal water samples from Banglazhang; ◇ geothermal water samples from Rehai; □ cold groundwater samples from Banglazhang.

In the δD vs. $\delta^{18}O$ plot (Fig. 3), all geothermal and cold spring samples collected from Banglazhang and its neighboring hydrothermal areas fall on or are close around the local rain water line, indicating their meteoric origin. Only three geothermal water samples show evident ^{18}O shifts, which should be induced by the ^{18}O exchange between geothermal waters and subsurface rocks at high temperatures as commonly observed elsewhere. As compared to the $\delta^{34}S$ values of sulfide, those of dissolved sulfate in the Banglazhang geothermal waters are highly variable. But the $\delta^{34}S$ values of sulfate in the Banglazhang samples are not significantly different from the samples collected from the other areas (Table 5). Nevertheless, the above conclusions need to be validated with further evidence in view of the limited available sulfur isotopic data. Moreover, in the $\delta^{34}S$-sulfate vs. $\delta^{34}S$-sulfide plot (Fig. 4), all Banglazhang samples are located in the area where the

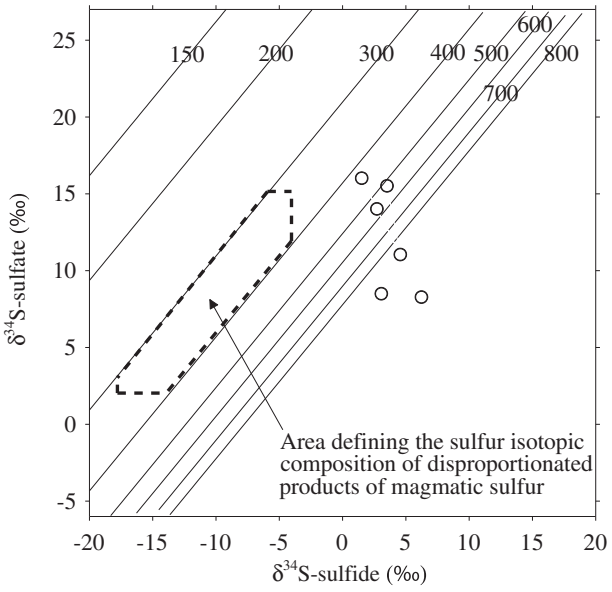

Fig. 4. Plot of $\delta^{34}S$-sulfate vs. $\delta^{34}S$-sulfide for the Banglazhang geothermal water samples. The lines indicate equilibrium between $\delta^{34}S$-sulfate and $\delta^{34}S$-sulfide, and the numbers denote temperatures (in °C) at which sulfur isotopic equilibrium is reached.

temperatures for sulfur isotopic equilibrium between sulfate and sulfide are greater than 400 °C, much higher than the subsurface temperatures estimated by solute geothermometers. It means that the sulfate in Banglazhang geothermal waters are generally far from isotopic equilibrium with coexisting sulfide, which is in accordance with the fact that the kinetics of ^{34}S exchange reaction is very slow as pointed out by Robinson (1973).

4.2. Evaluation of subsurface temperature and equilibrium status of geothermal water

Chemical geothermometers based on temperature-dependent change in solubility of individual minerals (e.g. quartz geothermometer) and exchange reactions concerning two or more minerals (e.g. Na-K or K-Mg geothermometer) are not only useful for reservoir temperature calculation, but also helpful for appraising the equilibrium status of geothermal waters and for identifying their geochemical genesis. For the Banglazhang geothermal springs, the subsurface temperatures estimated by use of Na-K (Giggenbach et al., 1983; Giggenbach, 1988), K-Mg (Giggenbach, 1988) and quartz (Verma and Santoyo, 1997) geothermometers (Table 6) are much higher than the sampling temperatures, and the temperatures calculated with K-Mg and quartz geothermometers are comparable but significantly lower than those with Na-K geothermometer. These differences suggest that K-Mg and quartz geothermometers reflect the geothermal water temperatures nearby spring outlet as they re-equilibrate very rapidly upon cooling with speeds close to each other, whereas Na-K geothermometer records the temperatures at greater depths.

A plot of the logarithm of SiO_2 against that of K^2/Mg ratio (Fig. 5) and a ternary Na-K-$Mg^{1/2}$ diagram (Fig. 6) for all Banglazhang geothermal water samples were also utilized to evaluate the ascending geothermal waters equilibrium status with respect to relevant minerals and the mixing processes they have experienced. In Fig. 5, some of the plotted samples were located on or very close to the SiO_2-K^2/Mg equilibrium curves, implying that the partial equilibrium of geothermal water with both common K-Mg minerals (such as K-feldspar, muscovite and chlorite) and certain SiO_2 mineral (either quartz or chalcedony) was attained. Nevertheless, the general disequilibrium situation of all Banglazhang geothermal waters is still clearly documented by the Na-K-$Mg^{1/2}$ diagram where they are located in partially equilibrated area or immature water area. The locations for the samples from Daheba, Dazhulin and Huangcaoba are similar to those of the Banglazhang samples, none of them being close to the full equilibrium line in Fig. 6. Hence, there is possibly a lack of geothermal fluids fully equilibrated with all major subsurface minerals in the hydrothermal systems investigated in this study.

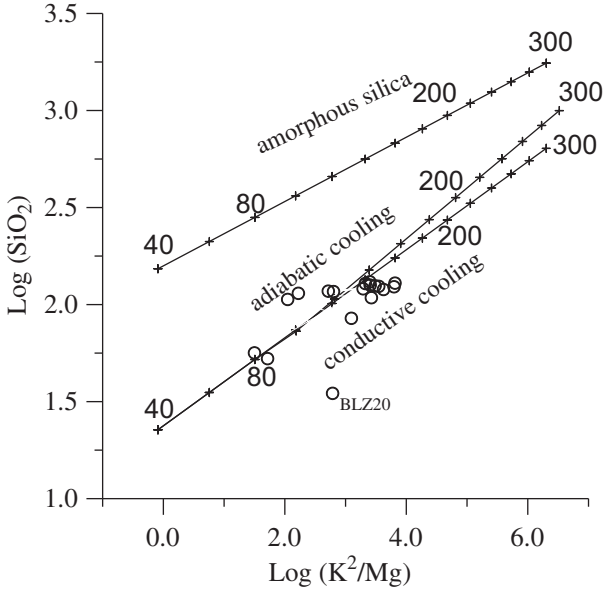

Fig. 5. Correlation plot of the logarithm of SiO_2 against that of K^2/Mg ratio for the Banglazhang geothermal water samples.

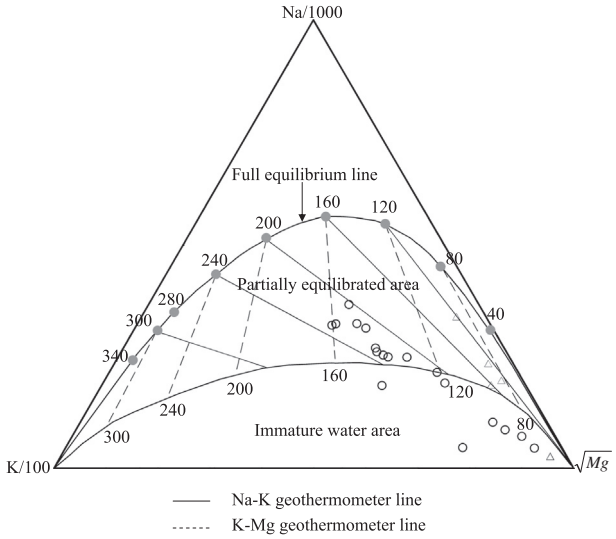

Fig. 6. Ternary diagram of Na-K-$Mg^{1/2}$ for geothermal water samples. Legend of sample symbols: ○ geothermal water samples from Banglazhang; Δ geothermal water samples from Daheba, Dazhulin and Huangcaoba.

The SiO_2-K^2/Mg plot also implies that there exists a shallow reservoir with temperatures near 150 °C in view that most data points conform to a nearly horizontal pattern that would intersect the equilibrium curves at a temperature of about 150 °C. We suggest that this shallow reservoir can be fed by a deeper, warmer geothermal fluid diluted by Ca- and Mg-rich cold groundwaters as indicated by the Cl-B-Ca and Cl-B-Mg plots (Fig. 7-a and 7-b, which will be discussed in detail later). The dilution causes the discordance between K-Mg and SiO_2 temperatures partly because the K-Mg geothermometer is more sensitive to such mixing than the SiO_2 geothermometers, which in turn results in the horizontal spread of the data points for most samples in Fig. 5. The Na-K-$Mg^{1/2}$ diagram (Fig. 6) shows that most Banglazhang geothermal samples have very close Na/K ratios corresponding to a Na-K temperature of about 220 °C, similarly indicating the mixing of reservoir geothermal waters with cold groundwaters. However, the actual temperature of this deep geothermal fluid endmember may even be higher than 220 °C because the Na-K geothermometer is very likely to be unreliable in this setting with partially equilibrated or immature waters. From the 150 °C shallow reservoir, the geothermal waters keep on ascending and form the hot springs at surface with a temperature range of 32 to 97 °C. During the ascent of geothermal waters, they should be controlled predominantly by conductive cooling (outpacing SiO_2 precipitation) as suggested by the very low discharges of the hot springs, so that most springs have comparable SiO_2 concentrations corresponding to a reservoir temperature of around 150 °C. A few samples with lower SiO_2 concentrations, e.g. BLZ20, may experience considerable near-surface dilution. In Fig. 5, sample BLZ20 is located far below the conductive cooling line, indicating a high mixing proportion of local cold water with low SiO_2 concentration.

4.3. Secondary processes affecting the geochemistry of geothermal waters

It is well documented that Cl and B are usually incompatible for alteration phases in natural water-rock environments. In fact they do not enter common rock-forming minerals and are not easily adsorbed by rock surface once leached from aquifer rocks (Ellis, 1970; Janik et al., 1991). This is also confirmed by the good correlation between Cl

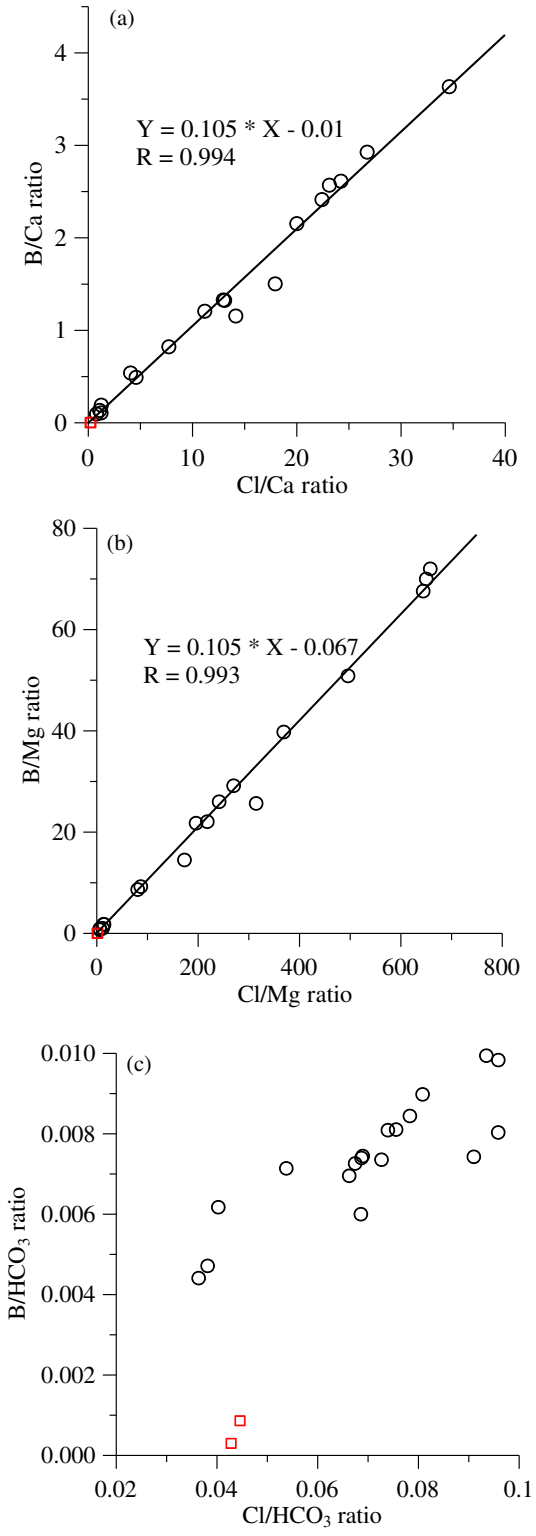

Fig. 7. Plots of B/Ca vs. Cl/Ca (a), B/Mg vs. Cl/Mg (b) and B/HCO_3 vs. Cl/HCO_3 (c) of Banglazhang water samples. The B/Ca-Cl/Ca and B/Mg-Cl/Mg plots indicate the mixing between geothermal waters and shallow cold groundwaters in the Banglazhang hydrothermal system. Legend of sample symbols: ○ geothermal water samples from Banglazhang; □ cold groundwater samples from Banglazhang.

and B in the Banglazhang geothermal waters. In contrast, the As to Cl ratios of Banglazhang geothermal waters are of a wider range than the B-Cl ratios. Although As is also claimed to be a conservative element (Ellis and Mahon, 1967), it acts compatibly in some sulfide-bearing alteration phases in hydrothermal environment where its concentration in

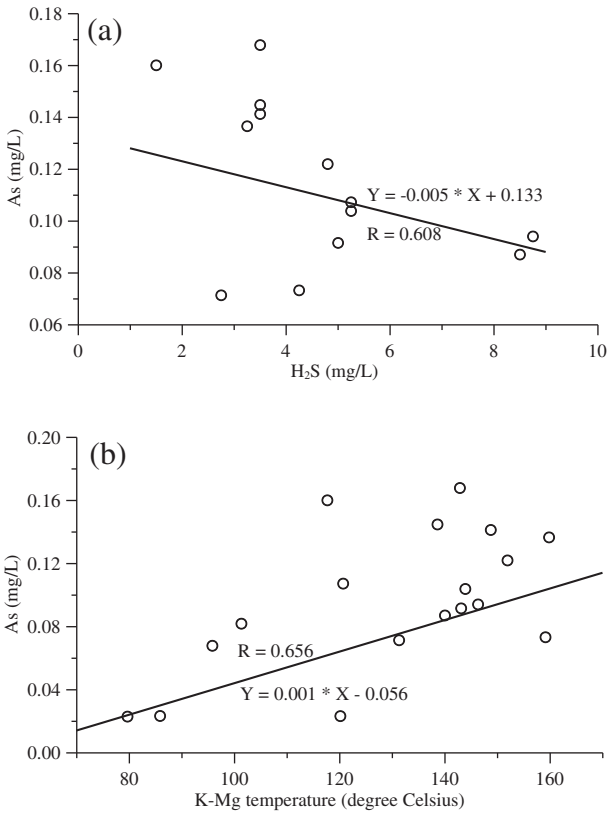

Fig. 8. Plots of As concentration vs. H_2S concentration (a) and K-Mg temperature (b) of the Banglazhang geothermal water samples.

geothermal water is controlled by both H_2S fugacity and reservoir temperature (Ballantyne and Moore, 1988). The As concentrations of Banglazhang geothermal waters show roughly negative and positive relations with the H_2S concentrations and K-Mg temperatures respectively (Fig. 8), in agreement with the arguments of Ballantyne and Moore (1988) that the interpretation of the trends in As/Cl ratio requires caution and there is usually no a common source or direct chemical association for As and Cl.

For Banglazhang geothermal samples, As concentrations and the molar ratios of most constituents change extensively revealing the effects of secondary processes occurring in the reservoirs, e.g. mixing with local cold groundwaters or precipitation of hydrothermally altered minerals. The mixing of Cl- and B-rich geothermal waters with Ca- and Mg-rich cold groundwaters below Banglazhang can be well illustrated by the B/Ca-Cl/Ca and B/Mg-Cl/Mg relations (Fig. 7-a and -b). For either of two diagrams, an excellent mixing line from the geothermal water endmember to the cold groundwater endmember can be drawn. All the geothermal water samples were clustered around the mixing lines, denoting their very similar Cl-B ratios and similar geochemical origin as mentioned above. In the B/HCO_3-Cl/HCO_3 diagram (Fig. 7-c), however, it is difficult to plot a mixing line between geothermal waters and cold groundwaters, possibly because the HCO_3^- concentrations of geothermal waters are also somewhat affected by the conversion of deeply-derived CO_2 at shallow levels where the subsurface temperatures are relatively low and thus the reactivity of CO_2 flowing upward along with geothermal water was strengthened. The effect of CO_2 on primary Ca-Al-silicates can result in the increase of bicarbonate and calcium concentrations which, sometimes, may cause further precipitation of secondary calcite as shown by Eqs. (4) and (5):

$$\text{Ca-Al-silicate} + 2CO_2 + 2H_2O = Ca^{2+} + 2HCO_3^- + 2(\text{H-Al-silicate}) \quad (4)$$

Table 7
Saturation indices of water samples with respect to calcite.

No.	SI_Calcite	No.	SI_Calcite	No.	SI_Calcite
BLZ01	0.439	BLZ11	0.109	DHB01	0.009
BLZ02	0.309	BLZ12	−0.572	DHB02	−0.057
BLZ03	0.191	BLZ13	−1.137	DZL01	−0.460
BLZ04	−0.135	BLZ14	0.300	HCB01	−0.192
BLZ05	0.073	BLZ15	−0.739	HCB02	−0.175
BLZ06	0.270	BLZ16	−0.416	HCB03	−0.241
BLZ07	−0.177	BLZ17	0.137	BLZ10c	0.379
BLZ08	−1.167	BLZ18	−0.450	BLZ19c	0.603
BLZ09	0.246	BLZ20	0.543	DZL02c	−1.231

$$Ca^{2+} + 2HCO_3^- = CaCO_3 + CO_2 + H_2O \quad (5)$$

The saturation indices of some Banglazhang geothermal springs with respect to calcite are calculated to be very close to zero (Table 7), indicating that secondary calcite was possibly formed at Banglazhang via alteration of Ca-Al-silicates as usually found in the high-temperature hydrothermal systems worldwide hosted by felsic rocks (Browne, 1978; White, 1986; Marini et al., 1998; Shen et al., 2011). Moreover, the Banglazhang samples can be divided into two groups according to their locations in the B/Ca-Cl/Ca and B/Mg-Cl/Mg diagrams. The group very close to the cold groundwater end member (including samples BLZ03, BLZ08, BLZ13, BLZ18 and BLZ20) was affected by mixing to higher degrees. It is interesting that all the samples in this group were collected further away from the Xiangbai River, whereas those less affected by mixing are located more adjacently to the river (see Fig. 1). Thus, the local cold groundwaters should be extensively distributed in the Xiangbai River valley. Their recharge source is the meteoric waters occurring in the nearby areas of the river. During the discharge of the cold groundwaters from relatively higher elevations to the river, they were mixed with ascending geothermal waters.

4.4. General discussion: geochemical genesis and heat source of Banglazhang geothermal waters

As discussed above, the Banglazhang geothermal field is marked by strong hydrothermal activities and high reservoir temperatures. However, the hydrochemical characteristics of geothermal waters sampled from Banglazhang are distinctively different from those occurring in magmatic-hydrothermal areas across the world. For a typical magmatic-hydrothermal system, three different types of hot springs are usually identified: acid SO_4-Cl (or Cl-SO_4) spring, neutral Cl spring and slightly alkaline to neutral HCO_3-Cl spring. At deep subsurface of such a system, the addition of magmatic fluids to infiltrating waters results in the formation of highly immature waters characterized by very high SO_4 concentration, comparatively high Cl concentration and very low pH value. The interactions between these immature acid waters and rocks, also called primary neutralization process (Giggenbach, 1988), can produce neutralized Cl waters, during which most magmatic sulfur are incorporated into alunite, anhydrite or pyrite at different depths. The chloride-dominant geothermal waters are commonly existent in mature magmatic-hydrothermal systems, such as the San Marcos hydrothermal area (Marini et al., 1998) in Guatemala, the Waiotapu hydrothermal area (Giggenbach et al., 1994) in New Zealand, and the Yangbajain hydrothermal area (Guo et al., 2007) and the Rehai hydrothermal area (Guo and Wang, 2012) in China. As the neutralized Cl waters ascend, they start to boil. Meanwhile a CO_2-rich vapor phase is probably formed and its reactivity can be enhanced by temperature decrease along the flow path of geothermal fluid. The conversion of CO_2 dissolved in neutral Cl waters to HCO_3^- via interaction with reservoir host rocks at comparatively shallow levels may generate HCO_3-Cl waters.

At Banglazhang, neutral Cl springs don't occur. All geothermal water samples collected from Banglazhang have high concentrations of HCO_3^- followed by comparable SO_4^{2-} and Cl^-. Their Cl concentrations (from 7.1 to 34.7 mg/L) are much lower than not only neutral Cl waters but also HCO_3-Cl waters formed in typical magmatic hydrothermal areas. Moreover, although the concentrations of B, As and Li in the Banglazhang geothermal waters are higher than the local cold groundwaters, they are generally much lower than high-temperature geothermal waters whose chemistry has been affected by magmatic fluid, such as those from Waiotapu (New Zealand), Guanacaste (Costa-Rica) and Yangbajain (China) (Giggenbach and Soto, 1992; Giggenbach et al., 1994; Guo et al., 2007). Provided that a magmatic heat source is existent below Banglazhang, a bold hypothesis for the geochemical genesis of the Banglazhang geothermal waters can be put forward that they are the result of mixing between acid SO_4-Cl or Cl-SO_4 waters, as a result of partial neutralization of magmatic fluids, and cold HCO_3 groundwaters at shallow levels. The high SO_4/Cl ratios of the Banglazhang geothermal waters, comparable to those of acid waters in active volcanic-hydrothermal areas, seem to be an evidence for the above speculation. The possibly existent acid fluids below Banglazhang should have much higher Cl, B, As and SO_4 concentrations as compared to those sampled at the surface, while upon mixing with shallow cold groundwaters, the concentrations of these constituents decrease sharply. The mixing process could not significantly change the B/Cl ratios of geothermal waters due to the low B and Cl concentrations of cold groundwaters. However, if the acid water exists in the Banglazhang system, its mixing ratio would be very low because the Cl concentrations of such acid waters are usually high. Assuming that the Cl concentration of the Banglazhang acid water is 3000 mg/L, the mixing ratio turns out to be less than 1%. Thus, the concentrations of Na in the acid water would be as high as more than 20,000 mg/L (the Na concentrations of the Banglazhang geothermal samples range from 59.8 to 213.7 mg/L), which is almost impossible to occur. Hence, although a mixing between deep geothermal water and shallow cold groundwater happens below Banglazhang as we have discussed, this geothermal water endmember is nothing to do with acid water formed through partial neutralization of magmatic fluid.

The stable O and H isotopes of the Banglazhang geothermal waters don't support the occurrence of magmatic fluid as well. Although slight ^{18}O shifts of geothermal water samples are observed, the likelihood is very small that they result from the addition of ^{18}O-rich magmatic fluid, a process that occurs commonly in active volcanic-hydrothermal areas. The geothermal waters sampled from the Rehai geothermal filed, a high-temperature field below which the input of magmatic fluid has been confirmed, are also plotted in the δD vs. $\delta^{18}O$ diagram (Fig. 3) for comparison. The ^{18}O shifts of Rehai samples, ranging from around 1 to 3‰, are much higher than those of Banglazhang samples. In fact, both oxygen-18 and deuterium contents of the Banglazhang geothermal waters are much more depleted than those of the Rehai geothermal waters. However, Rehai is marked by higher elevations (1390–1620 m) than Banglazhang (1260–1370 m), implying that the Rehai geothermal waters should have more depleted O and H isotopic composition. Thus, the addition of magmatic fluid enriched in D and ^{18}O, is very likely the process elevating the δD and $\delta^{18}O$ values of the Rehai geothermal waters. Based on the δD and $\delta^{18}O$ values of magmatic fluid given by Giggenbach (1992) (around −20‰ for δD and 10‰ for $\delta^{18}O$), the possible location of the Rehai water before its mixing with magmatic fluid should be at the lower left side of Fig. 3. Thus, the comparison with the Rehai geothermal waters shows that the isotopic compositions of the Banglazhang geothermal waters are unlikely affected by magmatic fluid.

The $\delta^{34}S$ values of sulfate and sulfide in the Banglazhang geothermal waters are also helpful for clarifying their geochemical genesis. To judge if magmatic sulfur contributes to the sulfur species in the Banglazhang geothermal waters, an area defining the plausible sulfur isotopic composition of disproportionated products of magmatic sulfur was plotted on the $\delta^{34}S$-sulfate vs. $\delta^{34}S$-sulfide diagram (Fig. 4) as per the following procedures. It is commonly accepted that SO_2 is the dominant sulfur

species in magmatic gases. In the volcanic gas samples collected from eleven active volcanoes across the world by Goff and McMurtry (2000), the molar proportions of SO_2 are generally much higher than those of H_2S. Sulfur occurs mainly as SO_2 in high-temperature magmatic fluids (higher than 400 °C) as well, as indicated by Holland (1965) based on thermodynamic calculations. However, at lower temperatures, SO_2 disproportionates into sulfate and sulfide species. Hence, the coexistence of aqueous sulfate and sulfide is usually one of the important factors controlling the redox status of geothermal water in magmatic-hydrothermal systems. In contrast, the dissolved SO_2 in geothermal water is usually negligible, as observed in the hydrothermal areas worldwide. In view that bisulfate ion is the prevailing sulfate species in acidic magmatic fluid, the disproportionation reaction of SO_2 can be expressed as below:

$$4SO_2 + 4H_2O \rightarrow H_2S + 3HSO_4^- + 3H^+ \quad (6)$$

The $\delta^{34}S$ values of abyssal magmatic sulfur are very close to that of Canyon Diablo Troilite (0‰) (Tong et al., 1982). For example, the $\delta^{34}S$ values of magmatic SO_2 from the Nevado del Ruiz Volcano (Colombia) are around 2.0‰ (Giggenbach et al., 1990). Thus, we can safely assume that the range of $\delta^{34}S$ values of magmatic sulfur is from −2‰ to 2‰, and the relation between the isotopic composition of original magmatic SO_2 and those of sulfate and sulfide as a result of disproportionation reaction can be written as follows:

$$\delta^{34}S_{SO_2} = \left[(n+2)\delta^{34}S_{SO_4} + (6-n)\delta^{34}S_{H_2S}\right]/8 \quad (7)$$

where $\delta^{34}S_{SO_2}$ is the isotopic composition of magmatic SO_2, and $\delta^{34}S_{SO_4}$ and $\delta^{34}S_{H_2S}$ those of disproportionated sulfate and sulfide. n denotes the oxidation state of magmatic SO_2 (equals to 4). By use of Eq. (7), the ranges of $\delta^{34}S$ values of disproportionated sulfate and sulfide at any specific temperature can be estimated.

However, magmatic sulfur may exist partly as H_2S as well. At this case, the Eq. (7) can be corrected as the following form:

$$\delta^{34}S_M = \left[(\overline{n}+2)\delta^{34}S_{SO_4} + (6-\overline{n})\delta^{34}S_{H_2S}\right]/8 \quad (8)$$

$\overline{n}$ is calculated using the equation below:

$$\overline{n} = n_{SO_2} \times R_{SO_2} + n_{H_2S} \times R_{H_2S} \quad (9)$$

where n_{SO_2} and n_{H_2S} are the oxidation states of SO_2 and H_2S (4 and −2 respectively), and R_{SO_2} and R_{H_2S} are the molar proportions of SO_2 and H_2S in magmatic sulfur. $\delta^{34}S_M$ is the isotopic composition of magmatic sulfur.

The lower limit of temperature necessary for occurrence of magmatic sulfur disproportionation is around 300 °C (Einaudi et al., 2003). Thus, presuming that the disproportionation of magmatic sulfur occurs at a temperature range of 300 to 400 °C and the ratio of H_2S in magmatic sulfur is between 0 and 0.5, the ranges of $\delta^{34}S$ values of sulfate and sulfide generated by disproportionation are calculated to be from 2.0‰ to 15.1‰ and from −17.8‰ to −4.0‰ respectively, as shown in Fig. 4. It is clear that the Banglazhang samples are outside the area in Fig. 4 plotted using the theoretic $\delta^{34}S$ ranges of sulfate and sulfide disproportionated from magmatic sulfur. Hence the sulfur species in the Banglazhang geothermal waters are not from magmatic fluid as well. Instead, the sulfur isotopic data of the Banglazhang geothermal water samples suggest that the H_2S in geothermal water possibly originate from the dissolution of sulfide minerals with $\delta^{34}S$ of +2‰ to +4‰. As a result of the oxidation of this H_2S to SO_4, the $\delta^{34}S$-sulfate values of the geothermal water samples are generally higher than 10‰. How the sulfide minerals themselves formed in the reservoirs is beyond the contents of this paper and cannot be discussed based on only the $\delta^{34}S$ data of surface geothermal waters.

Although both the hydrochemistry and the O, H and S isotopic compositions of Banglazhang geothermal waters are not affected by a magmatic fluid, it doesn't necessarily imply that there is no a magmatic heat source below Banglazhang. As introduced earlier, active geothermal manifestations characteristic for magma-heated hydrothermal systems, such as geyser and hydrothermal explosion, were observed at Banglazhang. More importantly, a seismic investigation showed that a volume of anomalously low P-wave velocity exists in the Wuhe-Longjiang area with comparatively shallow depths of 7–14 km (Lou et al., 2002). This geophysical anomaly below Wuhe-Longjiang, just about 10 km north to Banglazhang (Fig. 1-a), is speculated to be the reflection of a molten rock. Furthermore, the highest $^3He/^4He$ ratio for escaping geothermal gases from the Panzhihua hydrothermal area that is 20 km northwest to Banglazhang (Fig. 1-a) is 2.31 Ra, suggesting a mantle-derived magma intrusion into shallow crust below Panzhihua as well (Zhao, 2008). These geophysical and geochemical observations indicate that the Banglazhang hydrothermal system is likely to be located above the margin of a magma chamber whose center is possibly within the Wuhe-Longjiang-Panzhihua area. Thus, the Banglazhang hydrothermal system, with strong surface thermal manifestations and comparatively high subsurface temperatures, may still be a magma-heated system. Nevertheless, the Banglazhang geothermal waters are of a meteoric origin, and the dissolved constituents in water have no relations to a magmatic contribution but result from its reactions with subsurface rocks.

5. Conclusions

The geological genesis of the Banglazhang hydrothermal system, as inferred from the geochemical characteristics of geothermal springs, is substantially different from that of the Yangbajain system or the Rehai system where a direct contribution of magmatic fluid to geothermal water is existent. The parent geothermal liquids (PGL) in the deep reservoirs below Yangbajain and Rehai are neutral Cl waters in full equilibrium with reservoir minerals, which were formed upon a very long contact of strongly acidic magmatic fluid with subsurface rocks. In contrast, although there may exist a magma chamber below Banglazhang as implied by strong surface hydrothermal activities, high subsurface temperatures and geophysical observations, it seems that the Banglazhang geothermal waters are not affected by a magmatic fluid chemically; that is, there is no an input of magmatic fluid to the geothermal waters below Banglazhang. A mixing of deep geothermal waters with shallow cold groundwaters occurs in the Banglazhang system as indicated by the B/Ca-Cl/Ca and B/Mg-Cl/Mg diagrams, but this geothermal water endmember has nothing to do with an acidic, deep fluid released from magma chamber. This is also supported by the O, H and S isotopic data. Nevertheless, more investigations on the Banglazhang system, e.g. deep drilling or deep geophysical survey, are expected to be made for further verifying the conclusions reached in this study.

Acknowledgments

This study was financially supported by the National Natural Science Foundation of China (Nos. 41572335, 41120124003 and 41521001), the research program of China Power Investment Corporation (2015-138-HHS-KJ-X), and the research program of State Key Laboratory of Biogeology and Environmental Geology of China (GBL11505). The very helpful comments of two anonymous reviewers are gratefully acknowledged.

References

Bai, D.H., Liao, Z.J., Zhao, G.Z., Wang, X.B., 1994. The inference of magmatic heat-source beneath the rehai (hot sea) field of Tengchong from the result of magnetotelluric sounding. Chin. Sci. Bull. 39 (7), 572–577.

Ballantyne, J.M., Moore, J.N., 1988. Arsenic geochemistry in geothermal systems. Geochim. Cosmochim. Acta 52 (2), 475–483.

Browne, P.R.L., 1978. Hydrothermal alteration in active geothermal fields. Annu. Rev. Earth Planet. Sci. 6 (2), 229–250.
Coleman, M.L., Shepard, T.J., Durham, J.J., Rouse, J.E., Moore, G.R., 1982. Reduction of water with zinc for hydrogen analysis. Anal. Chem. 54 (1), 993–995.
Coplen, T.B., 1993. Normalization of oxygen and hydrogen isotope data. Chem. Geol. 72 (4), 293–297.
Duo, J., 2003. The basic characteristics of the Yangbajing geothermal field-A typical high temperature geothermal system. gerEng. Sci. 5 (1), 42–47.
Einaudi, M.T., Hedenquist, J.W., Inan, E.E., 2003. Sulfidation state of fluids in active and extinct hydrothermal systems: transitions from porphyry to epithermal environments. In: Simmons, S.F., Graham, I. (Eds.), Volcanic, Geothermal, and Ore-Forming Fluids: Rulers and Witnesses of Processes within the Earth 10. Society of Economic Geology Special Publication, pp. 285–313 (Chapter 15).
Ellis, A.J., 1970. Quantitative interpretation of chemical characteristics of hydrothermal systems. Geothermics 2, 516–527.
Ellis, A.J., Mahon, W.A.J., 1967. Natural hydrothermal systems and experimental hot water/rock interactions (Part II). Geochim. Cosmochim. Acta 31 (4), 519–538.
Giggenbach, W.F., 1988. Geothermal solute equilibria - derivation of Na-K-Mg-Ca geoindicators. Geochim. Cosmochim. Acta 52 (12), 2749–2765.
Giggenbach, W.F., 1992. Isotopic shifts in waters from geothermal and volcanic systems along convergent plate boundaries and their origin. Earth Planet. Sci. Lett. 113 (4), 495–510.
Giggenbach, W.F., Soto, R.C., 1992. Isotopic and chemical-composition of water and steam discharges from volcanic magmatic hydrothermal systems of the Guanacaste Geothermal Province, Costa-Rica. Appl. Geochem. 7 (4), 309–332.
Giggenbach, W.F., Gonfiantini, R., Jangi, B.L., Truesdell, A.H., 1983. Isotopic and chemical-composition of Parbati Valley geothermal discharges, Northwest Himalaya, India. Geothermics 12 (2–3), 199–222.
Giggenbach, W.F., et al., 1990. The chemistry of fumarolic vapor and thermal-spring discharges from the Nevado del Ruiz volcanic-magmatic-hydrothermal system, Colombia. J. Volcanol. Geotherm. Res. 42 (1-2), 13–39.
Giggenbach, W.F., Sheppard, D.S., Robinson, B.W., Stewart, M.K., Lyon, G.L., 1994. Geochemical structure and position of the Waiotapu geothermal-field, New-Zealand. Geothermics 23 (5-6), 599–644.
Goff, F., McMurtry, G.M., 2000. Tritium and stable isotopes of magmatic waters. J. Volcanol. Geotherm. Res. 97 (1-4), 347–396.
Guo, Q., Wang, Y., 2012. Geochemistry of hot springs in the Tengchong hydrothermal areas, Southwestern China. J. Volcanol. Geotherm. Res. 215, 61–73.
Guo, Q., Wang, Y., Liu, W., 2007. Major hydrogeochemical processes in the two reservoirs of the Yangbajing geothermal field, Tibet, China. J. Volcanol. Geotherm. Res. 166 (3–4), 255–268.
Guo, Q., Wang, Y., Liu, W., 2009. Hydrogeochemistry and environmental impact of geothermal waters from Yangyi of Tibet, China. J. Volcanol. Geotherm. Res. 180 (1), 9–20.
Holland, H.D., 1965. Some applications of thermochemical data to problems of ore deposits. II. Mineral assemblages and the composition of ore-forming fluids. Econ. Geol. 60 (1), 1101–1166.
Janik, C.J., et al., 1991. A geochemical model of the platanares geothermal system, Honduras. J. Volcanol. Geotherm. Res. 45 (1-2), 125–146.
Kharaka, Y.K., Mariner, R.H., 1989. Chemical geothermometers and their application to formation waters from sedimentary basins. In: Naeser, N.D., McCulloh, T.H. (Eds.), Thermal History of Sedimentary Basins. Springer, pp. 99–117.
Liao, Z., Zhao, P., 1999. Yunnan-Tibet Geothermal Belt-Geothermal Resources and Case Histories. Science Press, Beijing (in Chinese with English abstract).
Lin, H., Wang, S., Fu, H., 2006. Comprehensive analysis of underground fluid precursors for earthquake with the Banglazhang Hot Springs, Longling, Yunnan. Journal of Seismological Research 29 (1), 35–38.
Liu, Y., 2009. A Study of Geyser and Hydrochemistry of Thermal Groundwater in the Banglazhang Geothermal Field of Longling, Yunnan. China University of Geosciences (Beijing), Beijing (63 pp).
Lou, H., Wang, C., Huangpu, G., Qing, J., 2002. Three-demensional seismic velocity tomography of the upper crust in Tengchong volcanic area, Yunnan province. Acta Seismol. Sin. 24 (3), 243–251.
Marini, L., Cioni, R., Guidi, M., 1998. Water chemistry of San Marcos area, Guatemala. Geothermics 27 (3), 331–360.
Parkhurst, D.L., Appelo, C.A.J., 1999. A computer program for speciation, batch-reaction, one-dimensional transport, and inverse geochemical calculations. Water-Resources Investigations Report 99-4259. U.S. Geological Survey, Denver (312 pp).
Robinson, B.W., 1973. Sulphate-water and H2S isotope geothermometry in New Zealand geothermal systems. 4th International Conference of Geochronology, Cosmochronology and Isotope Geochemistry. U.S. Geological Survey, pp. 354–356 Open-File Report 78-701.
Shangguan, Z.G., Bai, C.H., Sun, M.L., 2000. Mantle-derived magmatic gas releasing features at the Rehai area, Tengchong county, Yunnan Province, China. Sci. China. Ser. D Earth Sci. 43 (2), 132–140.
Shen, L.C., Wu, K.Y., Xiao, Q., Yuan, D.X., 2011. Carbon dioxide degassing flux from two geothermal fields in Tibet, China. Chin. Sci. Bull. 56 (35), 3783–3793.
Tong, W., Zhang, M., 1989. Geothermics in Tengchong. Science Press, Beijing (262 pp).
Tong, W., Zhu, M., Chen, M., 1982. Sulfur-isotopic analysis and studies upon the Abyssal heat recharge of the Tibet's hydrothermal activities. Acta Sci. Nat. Univ. Pekin. 18 (2), 79–85.
Truesdell, A.H., Nathenson, M., Rye, R.O., 1977. The effects of subsurface boiling and dilution on the isotopic compositions of Yellowstone thermal waters. J. Geophys. Res. 82 (26), 3694–3704.
Verma, S.P., 2012. Geochemometrics. Revista mexicana de ciencias geológicas 29 (1), 276–298.
Verma, S.P., Santoyo, E., 1997. New improved equations for Na/K, Na/Li and SiO2 geothermometers by outlier detection and rejection. J. Volcanol. Geotherm. Res. 79 (1-2), 9–23.
Verma, S.P., Pandarinath, K., Santoyo, E., 2008. SolGeo: a new computer program for solute geothermometers and its application to Mexican geothermal fields. Geothermics 37 (6), 597–621.
White, A.F., 1986. Chemical and isotopic characteristics of fluids within the Baca Geothermal Reservoir, Valles Caldera, New-Mexico. J. Geophys. Res. Solid Earth Planets 91 (B2), 1855–1866.
Zhao, C.P., 2008. Mantle-derived Helium Release Characteristics and Deep Magmatic Activities in the Tengchong Volcanic Area. A dissertation for the Degree of Doctor of Philosophy. Institute of Geology, China Earthquake Administration, pp. 1–123.
Zhao, W., et al., 2002. Progress in the study of deep profiles (INDEPTH) in the Himalayas and Qinghai–Tibet Plateau. Geol. Bull. China 21 (11), 691–700.
Zhou, Z., Xiang, C., Zhao, Z., 1995. Characteristics of geothermal fields in western Yunnan. Journal of Seismological Research 18 (1), 41–48.